

## Localized measurements of the fast ion velocity distribution of TEXTOR plasmas using collective Thomson scattering

D. Moseev<sup>1</sup>, S.B. Korsholm<sup>1</sup>, F. Meo<sup>1</sup>, S.K. Nielsen<sup>1</sup>, H. Bindslev<sup>1</sup>, A. Bürger<sup>2</sup>, E. Delabie<sup>3</sup>, V. Furtula<sup>1</sup>, M.Yu. Kantor<sup>2,3,4</sup>, T. Koskela<sup>5</sup>, F. Leipold<sup>1</sup>, P.K. Michelsen<sup>1</sup>, M. Salewski<sup>1</sup>, O. Schmitz<sup>2</sup>, M. Stejner<sup>1</sup>, R. Uhlemann<sup>2</sup>, E. Westerhof<sup>3</sup> and the TEXTOR team<sup>2</sup>

<sup>1</sup> EURATOM-Risø DTU, Technical University of Denmark, DK-4000 Roskilde, Denmark

<sup>2</sup> FZ Jülich GmbH, EURATOM, Trilateral Euregio Cluster, D-52425 Jülich, Germany

<sup>3</sup> FOM-IPP, EURATOM, PO Box 1207, 3430 BE Nieuwegein, The Netherlands

<sup>4</sup> Ioffe Institute, RAS, Saint Petersburg 194021, Russia

<sup>5</sup> Aalto University, EURATOM-TEKES, P.O. Box 15100 FI-00076 AALTO, Finland

### Introduction

Fast ion physics is of importance to nuclear fusion. Therefore measurements of the fast ion velocity distribution function at different locations in the plasma volume will be of significant value. There are a number of diagnostics on present devices which can detect fast ions, e.g. fast ion D $\alpha$  spectroscopy (FIDA) [1],  $\gamma$ -ray spectroscopy [2], scintillator probes [3] and collective Thomson scattering (CTS) [4]. They do not replace but rather complement each other. For CTS, fast ion information is inferred from probe radiation scattered from electron density fluctuations in the plasma. When the wavelength of the fluctuations is much larger than the Debye length ( $L_D \cdot k^\delta \ll 1$ ), the scattered signal is mainly due to collective effects in the plasma. Here  $\vec{k}^\delta$  is a fluctuation wave vector defined by  $\vec{k}^\delta = \vec{k}^s - \vec{k}^i$ , where  $\vec{k}^s$  and  $\vec{k}^i$  represent the wave vectors of scattered and incident radiation respectively. The scattered signal comes from the volume determined by the overlap of the probe and receiver beams. The 1D fast ion distribution function is inferred by fitting the spectrum through a Bayesian procedure using a forward model for scattering [5]. The CTS diagnostic on the TEXTOR tokamak is equipped with a steerable mirror system which enables measurements of 1D projections of the fast ion distribution function along  $\vec{k}^\delta$  at different radial positions in the plasma and at different angles  $\phi = \angle(\vec{B}, \vec{k}^\delta)$  to the magnetic field. Results presented in this paper are obtained for the plasma center at  $R \approx 1.8$  m and off-axis at  $R \approx 2.0$  m at two different pitch angles  $\phi \approx 140^\circ$  and  $\phi \approx 110^\circ$ .

### Setup

The experiments presented here were conducted in deuterium plasmas with hydrogen NBI in the TEXTOR tokamak ( $R = 1.75$  m,  $a = 0.47$  m). Fast ions come from the co- $I_P$  neutral beam injector at 1.2 MW with acceleration voltage of 50 keV. The TEXTOR neutral beam injectors

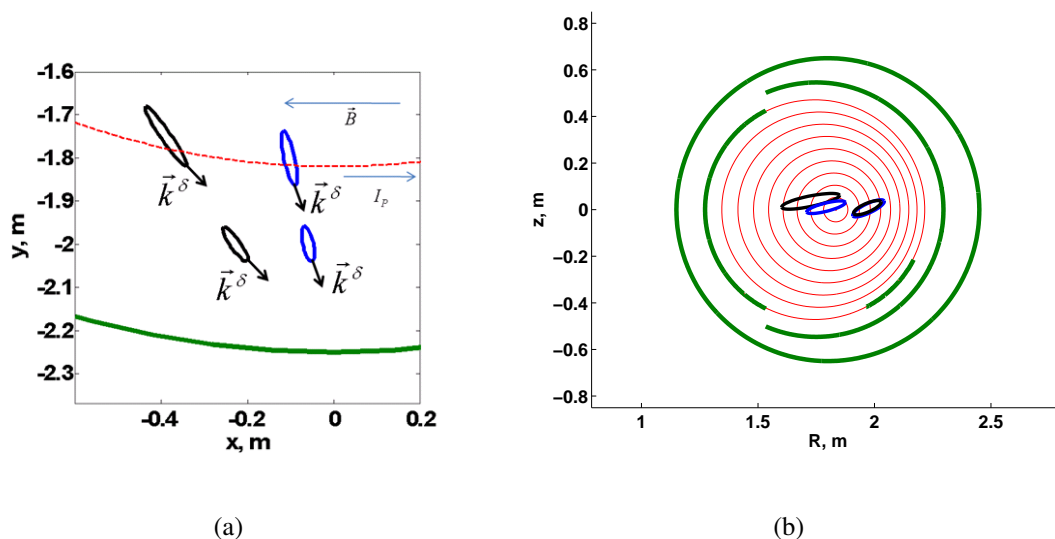


Figure 1: Geometry of the experiments. (a) Top view showing the plasma center (red) and the LFS limiter (green); (b) Poloidal view showing estimated flux surfaces (red) and limiters and the vacuum vessel (both in green). The blue and black ellipsoids in both figures denote the measurement volumes, where black corresponds to  $\phi \approx 140^\circ$  and blue to  $\phi \approx 110^\circ$

are very tangential. The tangential radius (the radius at which the injected beam is parallel to the magnetic field) is 1.65 m. A high power microwave beam (180 kW) in ordinary mode at 110 GHz was launched into the plasma and scattered radiation is detected by the CTS receiver [6] also in the ordinary mode.

## Experiment

The received signal consists of scattered radiation and ECE background. In order to distinguish between them, the gyrotron is modulated. In this experiment 2 ms bursts of radiation are launched periodically every 20 ms. In order to find the antenna position that corresponds to maximum overlap, we swept the receiver beam across the gyrotron beam. The signal strength during such an experiment changes with the overlap and has a bell-like shape as a function of time. The procedure of overlap sweeps is discussed in detail in [7]. We conducted experiments at different radial positions and pitch angles. The geometry of the experiments is illustrated in Fig. 1.

We made measurements during four overlap sweeps in four reproducible discharges with  $I_p = 400$  kA,  $B_T = 2.6$  T. Such a field is essential to position the fundamental and the second harmonic of electron-cyclotron resonance at the gyrotron frequency outside the plasma in order to avoid absorption of the gyrotron power and to minimize the ECE background. Plasma param-

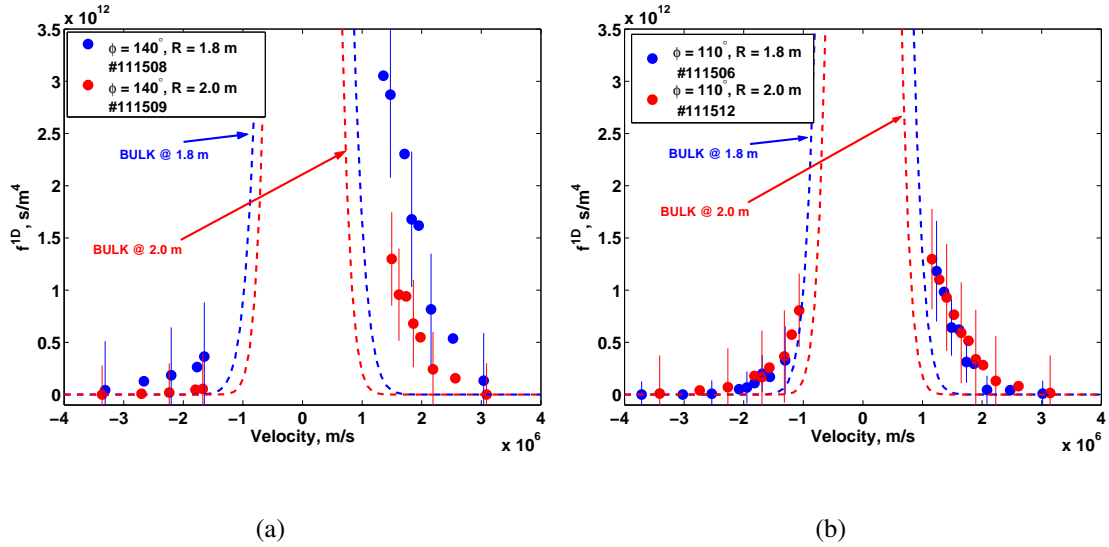


Figure 2: 1D projections of fast ions velocity distribution functions to  $\vec{k}^\delta$  direction at different radial positions ( $R = 1.8 \text{ m}$  - blue;  $R = 2.0 \text{ m}$  - red). (a)  $\phi \approx 140^\circ$ ; (b)  $\phi \approx 110^\circ$ . The bulk features in both graphs are calculated with CXRS data.

ters at the center ( $\rho = 0$ ) were:  $n_e = 3.5 \cdot 10^{19} \text{ m}^{-3}$ ,  $T_e = 1.7 \text{ keV}$ ,  $T_i = 2.7 \text{ keV}$  with co- $I_p$  NBI at  $1.2 \text{ MW}$ .

During the experiments, the plasma was sawtoothing. In order to avoid any influence of anisotropic fast ion redistribution [8], the gyropulses analyzed were taken right before a sawtooth crash and still in the time window with sufficient overlap during the sweep.

## Results and discussion

The measured signal in the CTS diagnostic is the scattered spectrum. The fast ion distribution function was inferred through fitting the experimental spectrum with one predicted by a model for CTS. We use the model described in [9] and Bayesian least squares fitting procedure which accounts for nuisance parameters (LSN). The *nuisance parameters* are defined as parameters which the CTS spectrum depends on ( $T_e$ ,  $T_i$ , scattering angle, etc) but which are not the parameters of interest (i.e. fast ion velocity distribution). The main difference between LSN and the least squares fitting is that LSN can treat nuisance parameters either as free or fixed and take uncertainties in them into account. Therefore we can make full use of prior information about all relevant model parameters. The inferred 1D velocity distribution functions are shown in Fig. 2. The errorbars in the velocity distribution functions account for one standard deviation of the spectral power density of a single gyrotron burst. These errorbars also take into account uncertainties of plasma parameters which influence scattered spectrum:  $T_e$ ,  $T_i$ ,  $n_e$ ,  $V_{rot}$ , etc.

Positive velocities in the distribution function corresponds to the direction along  $\vec{k}^\delta$ . According to Fig. 1(a), the toroidal component of  $\vec{k}^\delta$  is in the same direction of  $I_p$  and thus with the direction of neutral beam injection. One can see strong anisotropy of the distribution functions at  $\phi \approx 140^\circ$  (Fig. 2(a)) which is consistent with our expectations due to very tangential geometry of the neutral beam injection. Even though the difference in pitch angles in the experiment was only about  $30^\circ$  the anisotropy in the distribution functions at  $\phi \approx 110^\circ$  (Fig. 2(b)) is much more weakly pronounced than in the case of  $\phi \approx 140^\circ$  scattering geometry. It is important to notice that the difference in the distribution function shapes in Fig. 2(a) ( $\phi=140^\circ$ ) is distinguishable within the diagnostic accuracy. Fig. 2 shows some degree of inhomogeneity, hence has some information of the fast ion pressure profile which should be compared to Monte Carlo simulations. Future work will seek to improve the accuracy of the inferred fast ion velocity distribution function. Comparison of these measurements with numerical Monte Carlo simulations is on-going and the results of this comparison will be reported in a separate article.

## References

- [1] M. Van Zeeland and et al. *PPCF*, 51(5):055001, 2009.
- [2] Kiptily V.G. and et al. *Nuclear Fusion*, 45(5):L21–L25, 2005.
- [3] M. Nishiura and et al. *RSI*, 75(10):3646, 2004.
- [4] S. Michelsen and et al. *RSI*, 75(10):3634, 2004.
- [5] H. Bindslev. *RSI*, 70:1093–1099, 1999.
- [6] S. B. Korsholm and et al. *RSI*, 77, 2006.
- [7] Nielsen S. K. and et al. *Physical Review E*, 77:016407, 2008.
- [8] Nielsen S. K. et al. *submitted to PPCF*, 2010.
- [9] H. Bindslev. PhD thesis, Risø National Laboratory, Roskilde, Denmark, 1992.